

Experimental Study of Fluxon Dynamics in a Potential Well

Alexey V. Ustinov and Norbert Thyssen

*Institute of Thin Film and Ion Technology, Research Center (KFA)
D-52425 Jülich, Germany*

Dynamics of a single fluxon in an annular Josephson junction is studied in the presence of an externally applied magnetic field H . Due to the interaction of the fluxon with the radial field component, the fluxon moves in a potential well which height is proportional to H . Several spectacular features of fluxon dynamics analogous to the motion of a particle in a washboard potential are clearly observed experimentally. Periodic revolutions of the fluxon in the junction lead to a potential induced emission of plasma waves. These waves are indicated by a resonance at a certain fluxon velocity which depends on the junction length. Good agreement between experiment, theoretical model and numerical simulations is found.

PACS numbers: 74.50.+r, 03.40.Kf, 03.65.pm

1. INTRODUCTION

Due to the magnetic flux quantization in a superconducting ring, the number of fluxons (Josephson vortices) initially trapped in an annular junction is conserved. The fluxon dynamics can be studied here in the absence of system boundaries, i.e. under periodic boundary conditions. While the fabrication of annular Josephson tunnel junctions is rather easy, trapping of fluxons in them remains the state of art. Using different trapping techniques, both single-fluxon¹ and multi-fluxon^{2,3} dynamics have been investigated in homogeneous junctions.

We report here new experiments with annular Josephson junctions. In contrast to previous studies, a modified sample design and high homogeneity of the tunnel barrier allow to trap fluxons in the junction in a well control-

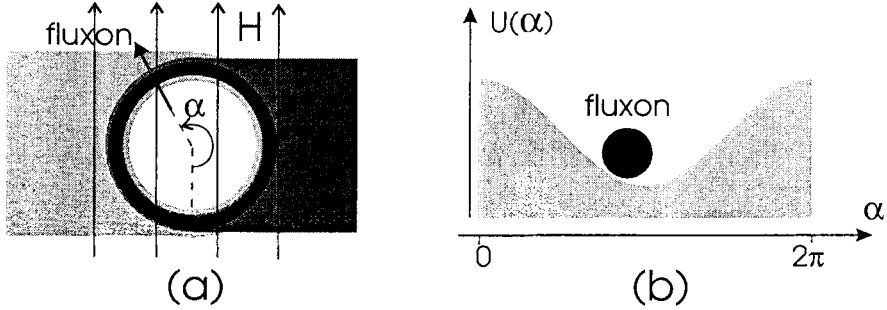


Fig. 1. (a) Schematic view of an annular junction (dimensions not to scale) with trapped fluxon; a magnetic field H is applied in the plane of the tunnel barrier. (b) An effective potential for the fluxon in the junction at zero bias current, the potential height is proportional to H .

lable way. We study the dynamics of a single fluxon in the presence of an externally applied magnetic field H . Due to the interaction of the fluxon with the radial field component, the fluxon moves in a potential with the amplitude proportional to H . The geometry as well as the fluxon potential profile are schematically shown in Fig. 1. The potential minimum is located in the region of the ring where the fluxon is directed along the field.

The model for an annular Josephson junction placed in the magnetic field was proposed by Grønbech-Jensen, Lomdahl, and Samuelsen.⁴ They showed that the field accounts for an additional term in the perturbed sine-Gordon equation which describes the system:

$$\varphi_{xx} - \varphi_{tt} = \sin \varphi + \alpha \varphi_t - \gamma - h \sin \frac{2\pi x}{\ell}, \quad (1)$$

where $\varphi(x, t)$ is a superconducting phase difference between the electrodes of the junction, the spatial coordinate x is normalized to the Josephson penetration depth λ_J , the time t is normalized to the inverse plasma frequency ω_0^{-1} , α is the dissipation coefficient due to the quasiparticle tunnelling through the tunnel barrier, γ is the bias current density normalized to the critical current density J_c of the junction, $\ell = \pi D / \lambda_J$, D is the ring diameter. The last term in Eq. (1) accounts for the coupling between the applied field and the flux density in the junction. The dimensionless amplitude $h \propto H$ is normalized by a sample-specific geometrical factor.^{4,5} Eq. (1) is accompanied by the periodic boundary conditions:

$$\varphi(\ell) = \varphi(0) + 2\pi ; \quad \varphi_x(\ell) = \varphi_x(0), \quad (2)$$

which assume that there is one fluxon in the ring.

So far, only *static* effects related to fluxon pinning have been studied in annular junctions placed in external magnetic field.^{5,6} Here we investigate experimentally the *dynamics* of such systems, in particular, trapping of a moving fluxon by the field-induced potential and resonance effect due to the fluxon interaction with the emitted radiation.

At *low velocities* the fluxon dynamics is similar to that of a driven pendulum in the presence of losses.⁷ By analogy with a small underdamped Josephson junction (without any spatial extension), the fluxon force-velocity (current-voltage, $I-V$) characteristic exhibits a hysteresis corresponding to the difference between the maximum pinning current I_{cr} and the threshold return current I_{tr} at which the fluxon gets trapped by the field-induced potential. Interestingly, the effective "Stewart-McCumber parameter"^{8,9} which determines this hysteresis depends here on the length of the junction ℓ . At *high velocities* the single-particle mechanical analogy breaks down and the fluxon experiences large energy losses due to the emission of plasma waves which occur due to the presence of the field-induced potential. The characteristic frequency of radiated waves leads to a sharp resonance on $I-V$ characteristics. The strength of this resonance can be changed by the height of the potential, i.e. by the external magnetic field.

2. EXPERIMENTAL RESULTS

2.1. Samples

Experiments have been performed with Nb/Al-AlO_x/Nb Josephson junctions of the classical annular geometry¹ schematically shown in Fig. 1(a). Trapping of a magnetic flux in the junction ring was made while cooling the sample below the critical temperature $T_c^{\text{Nb}} = 9.2$ K of niobium. Measurements were performed by applying the bias current I from top to the bottom electrode of the junction and measuring the dc voltage generated due to the fluxon motion. Results presented below were obtained with a junction with the mean diameter $D = 132 \mu\text{m}$ and the ring width $W = 10 \mu\text{m}$. In the investigated temperature range from $T = 4.2$ K to $T = 7.3$ K the normalized junction circumference ℓ varied between 8.1 and 7.7.

2.2. Fluxon Activation and Trapping in the Field-induced Potential

Current-voltage characteristics of one fluxon in the annular junction with no field applied have shown a very small zero-voltage current $I_{\text{cr}}(0)$, by factor of about 300 smaller than the critical current I_c measured for the same junction without trapped fluxon. Such an negligible fluxon pinning

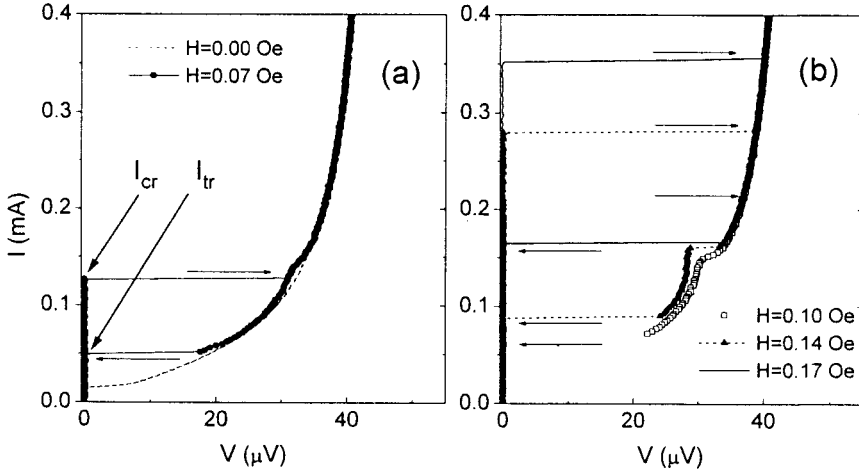


Fig. 2. Current-voltage characteristics of a single fluxon revolving in an annular Josephson junction at $T = 7.3$ K at different applied magnetic field H indicated on the plots.

indicated very high homogeneity of the junction.

Figure 2(a) presents one-fluxon $I - V$ curves measured with and without the external magnetic field H applied in the plane of the junction. At $H \neq 0$ the current I_{cr} increases and the hysteresis appears on the $I - V$ curve. As long as $V = 0$, the fluxon remains pinned in the potential produced by the applied field H . At $I > I_{cr}$ it overcomes the potential barrier and starts to revolve in the junction, thereby generating a dc voltage. If the current is decreased from here on, the fluxon motion continues ($V \neq 0$) until the current is low enough for the fluxon to be trapped by the field-induced potential well. The return current at which the junction switches to $V = 0$ we call the trapping current, I_{tr} . Both I_{cr} and I_{tr} were found to be strongly dependent on the applied field as discussed in Sec. 3.1.

2.3. Resonance Between Fluxon and Emitted Radiation

With increasing further the magnetic field H we observed a new resonance on $I - V$ characteristics, as presented in Fig. 2(b). While decreasing the bias current on the main step, the $I - V$ curves shows the resonant step at about 37μ V. The shape of this step strongly depends on the temperature and the applied field H . As discussed in more detail in the following section, the step is due to a resonance between moving fluxon and its radiation which occurs due to the field-induced potential in the junction. At low temperatures we observed this resonant step to become much more complicated

showing negative differential resistance and chaotic switching between several closely located branches. The complex shape of such resonance was predicted theoretically⁷ and can be attributed to a strong fluxon-plasma wave interaction which leads to an intrinsically chaotic dynamics in the junction.

3. DISCUSSION

3.1. Fluxon Pinning and Trapping

Using the theoretical model⁴ given by Eq. (1), both the critical current I_{cr} and the trapping current I_{tr} can be calculated in the adiabatic limit for $h \ll 2\pi/\ell$. The zero-voltage state is stable as long as the maximum pinning force of the potential F_{max} is larger than the force of the bias current acting on the fluxon. This can be satisfied⁴ in the range $|\gamma| < \gamma_{\text{cr}}$ where

$$\gamma_{\text{cr}} = h \operatorname{sech} \frac{\pi^2}{\ell}. \quad (3)$$

Thus, $I_{\text{cr}} = \gamma_{\text{cr}} I_c / (\pi DW)$ is expected to be proportional to H .

Grønbech-Jensen et al.⁷ have shown that in the low-velocity limit $v^2 \ll 1$ the fluxon as a particle can be described by the equation of motion

$$\ddot{\xi} + \alpha \dot{\xi} + \frac{\pi}{4} \gamma = \frac{\pi}{4} \gamma_{\text{cr}} \sin \frac{2\pi\xi}{\ell}, \quad (4)$$

where ξ is the fluxon coordinate. Eq. (4) is the equation of motion for the damped and driven pendulum. It is also well-known for describing the dynamics of a conventional small Josephson junction. The fluxon coordinate in the system discussed here is analogous to the phase variable of a small junction. Thus, the trapping current γ_{tr} here is determined by the analog of the Stewart-McCumber parameter^{8,9} for this system. In the non-relativistic case $v^2 \ll 1$ it can be calculated as¹⁰

$$\gamma_{\text{tr}} = \frac{8\alpha}{\pi^2} \sqrt{\frac{h\ell}{2} \operatorname{sech} \frac{\pi^2}{\ell}}. \quad (5)$$

We have measured the currents I_{cr} and I_{tr} as a function of the magnetic field H . Results obtained at $T = 5.9$ K are shown by data points in Fig. 3. The ratio between h and H is obtained by fitting the experimentally measured dependence $I_{\text{cr}}(H)$ to Eq. (3). In order to determine α in the experiment, we analyzed the form of the $I - V$ curves measured at $H = 0$. We used the fitting procedure for the V^{-2} vs I^{-2} diagram¹ which relies on the soliton force-velocity relation¹¹

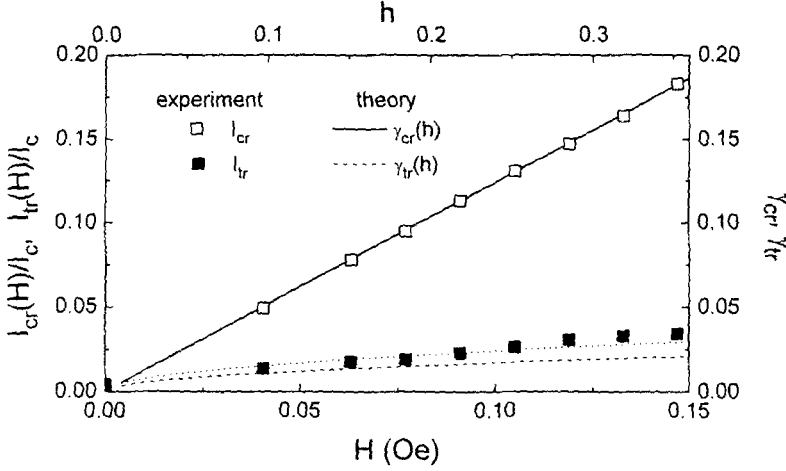


Fig. 3. Measured critical current I_{cr} and trapping current I_{tr} versus the applied magnetic field H at $T = 5.9$ K. The lines show the theoretically predicted dependence given by Eq. (3) (solid line) and Eq. (5) using the experimentally evaluated value for the damping parameter $\alpha = 0.030$ (dashed line) and $\alpha = 0.043$ (dotted line).

$$\frac{1}{\gamma^2} = \left(\frac{\pi}{4\alpha} \right)^2 \left(\frac{1}{v^2} - 1 \right) \left[1 + \frac{\beta}{3\alpha(1-v^2)} \right]^{-2}. \quad (6)$$

where β is the surface loss coefficient, not included in Eq. (1) for the sake of simplicity. The β loss term is mostly relevant for high soliton velocities, while at low velocities it can be approximated by the effective loss parameter $\alpha_{eff} \approx \alpha + \beta/3$. For the temperature $T = 5.9$ K we obtained $\alpha_{eff} = 0.030$. The dashed line in Fig. 3 is drawn according to Eq. (5) using the experimentally obtained loss coefficient $\alpha = \alpha_{eff}$. Though a better fit can be obtained with somewhat larger $\alpha = 0.043$, the experimentally found $I_{tr}(H)$ dependence rather well agrees with the theoretical prediction. For the higher fields $H > 0.2$ Oe we found a striking discrepancy between the theory and experiment which showed considerably higher I_{tr} than that predicted by Eq. (5). This discrepancy is attributed to the resonance effect discussed below.

3.2. Radiation and Resonance Effect

At sufficiently large H the fluxon strongly interacts with the field-induced potential in the junction, and a large part of fluxon's energy is transferred into the radiation of plasma waves. A fluxon rotating in an annular junction can be viewed as a soliton moving in a periodic potential

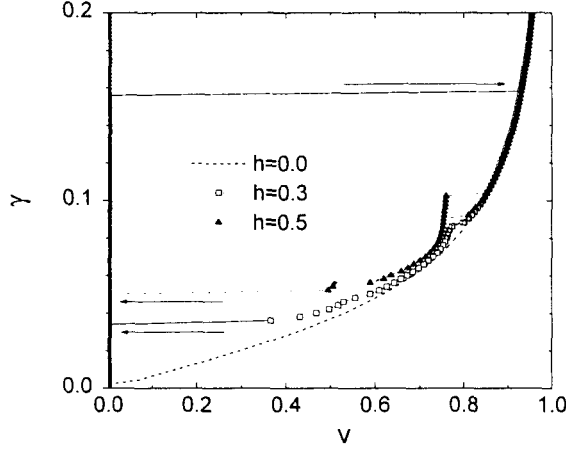


Fig. 4. Numerically simulated current-voltage characteristics of a single fluxon in the annular junction with parameters $\ell = 7.8$, and $\alpha \approx 0.05$. The resonant step associated with the interaction of the moving fluxon with the radiation is seen at $v \approx 0.75$.

which has a spatial period of πD . Under such conditions, the soliton is predicted to emit plasma waves which frequency depends on the period of the potential and the soliton velocity.¹² The presence of the radiation with given frequency should lead to a resonance which appears as an additional step on $I - V$ characteristics.¹³

We have simulated the current-voltage curves γ vs v numerically by integrating Eq. (1) with the boundary conditions (2). The simulation results for $\ell = 7.8$ and $\alpha = 0.05$ are presented in Fig. 4. One can see that the qualitative agreement between the simulations and the experimental data of Fig. 2(b) is very good. Some features of the internal dynamics of the junction corresponding to the simulated $\gamma(v)$ characteristics are shown in Fig. 5. One can see that the resonant step at $v \approx 0.75$ is characterized by the background oscillations (plasma waves) with the period 3 times smaller than the fluxon oscillations period. A detailed experimental and theoretical study of this resonance effect will be published elsewhere.¹⁴

ACKNOWLEDGMENT

The authors are grateful to Boris Malomed for valuable discussions.

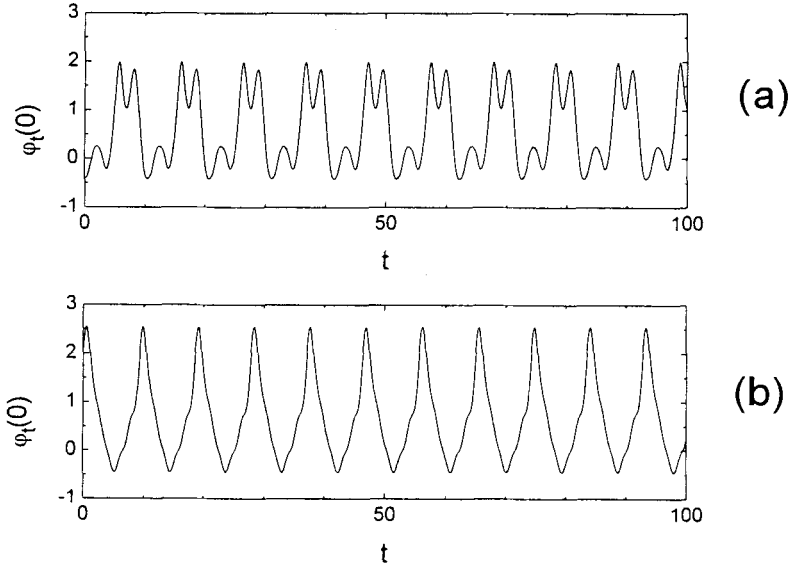


Fig. 5. Voltage oscillations at different points of $\gamma(v)$ curve shown in Fig. 4 for $h = 0.5$: (a) at the potential-induced resonant step for $\gamma = 0.09$ and $v = 0.75$; (b) at the main fluxon step for $\gamma = 0.10$ and $v = 0.84$.

REFERENCES

1. A. Davidson, B. Dueholm, B. Kryger, and N. F. Pedersen, *Phys. Rev. Lett.* **55**, 2059 (1985).
2. A. V. Ustinov, T. Doderer, R. P. Huebener, N. F. Pedersen, B. Mayer, and V. A. Oboznov, *Phys. Rev. Lett.* **69**, 1815 (1992).
3. I. V. Vernik, N. Lazarides, M. P. Sørensen, A. V. Ustinov, N. F. Pedersen, and V. A. Oboznov, *J. Appl. Phys.* **79**, 7854 (1996).
4. N. Grønbech-Jensen, P. S. Lomdahl, and M. R. Samuelsen, *Phys. Lett. A* **154**, 14 (1991).
5. N. Martucciello and R. Monaco, *Phys. Rev. B* **53**, 3471 (1996).
6. I. V. Vernik, S. Keil, N. Thyssen, T. Doderer, A. V. Ustinov, H. Kohlstedt, and R. P. Huebener, submitted to *Phys. Rev. B* (May 1996).
7. N. Grønbech-Jensen, P. S. Lomdahl, and M. R. Samuelsen, *Phys. Rev. B* **43**, 12799 (1991).
8. W. C. Stewart, *Appl. Phys. Lett.* **12**, 277 (1968).
9. D. E. McCumber, *J. Appl. Phys.* **39**, 3113 (1968).
10. B. A. Malomed, unpublished.
11. D. W. McLaughlin and A. C. Scott, *Phys. Rev. A* **18**, 1652 (1978).
12. G. S. Mkrtchyan and V. V. Schmidt, *Solid St. Commun.* **30**, 791 (1979).
13. A. A. Golubov, A. V. Ustinov, and I. L. Serpuchenko, *Phys. Lett. A* **130**, 107 (1988).
14. A. V. Ustinov, unpublished.